

# Nanoscale

Accepted Manuscript



This is an *Accepted Manuscript*, which has been through the Royal Society of Chemistry peer review process and has been accepted for publication.

*Accepted Manuscripts* are published online shortly after acceptance, before technical editing, formatting and proof reading. Using this free service, authors can make their results available to the community, in citable form, before we publish the edited article. We will replace this *Accepted Manuscript* with the edited and formatted *Advance Article* as soon as it is available.

You can find more information about *Accepted Manuscripts* in the [Information for Authors](#).

Please note that technical editing may introduce minor changes to the text and/or graphics, which may alter content. The journal's standard [Terms & Conditions](#) and the [Ethical guidelines](#) still apply. In no event shall the Royal Society of Chemistry be held responsible for any errors or omissions in this *Accepted Manuscript* or any consequences arising from the use of any information it contains.

Cite this: DOI: 10.1039/c0xx00000x

www.rsc.org/xxxxxx

**ARTICLE TYPE**

# Plasma-Assisted Quadruple-Channel Optosensing of Proteins and Cells with Mn-Doped ZnS Quantum Dots

Chenghui Li, Peng Wu,\* Xiandeng Hou\*

*Received (in XXX, XXX) Xth XXXXXXXXXX 20XX, Accepted Xth XXXXXXXXXX 20XX*

DOI: 10.1039/b000000x

Information extraction from nano-bio-systems is crucial for understanding their inside molecular level interactions and can help with developing multidimensional/multimodal sensing devices to realize novel or expanded functionalities. The intrinsic fluorescence (IF) of proteins has long been considered as an effective tool for studying protein structure and dynamics, but not for protein recognition analysis partially because it generally contributes to the fluorescence background in bioanalysis. Here we explored the use of IF as the fourth channel optical input for a multidimensional optosensing device, together with the triple-channel optical output of Mn-doped ZnS QDs (fluorescence from ZnS host, phosphorescence from Mn<sup>2+</sup> dopant, and Rayleigh light scattering from the QDs), to dramatically improve the protein recognition and discrimination resolution. To further increase the cross-reactivity of the multidimensional optosensing device, plasma modification of proteins was explored to enhance the IF difference as well as their interactions with Mn-doped ZnS QDs. Such a sensor device was demonstrated for highly discriminative and precise identification for proteins in human serum and urine samples, and for cancer and normal cells as well.

## Introduction

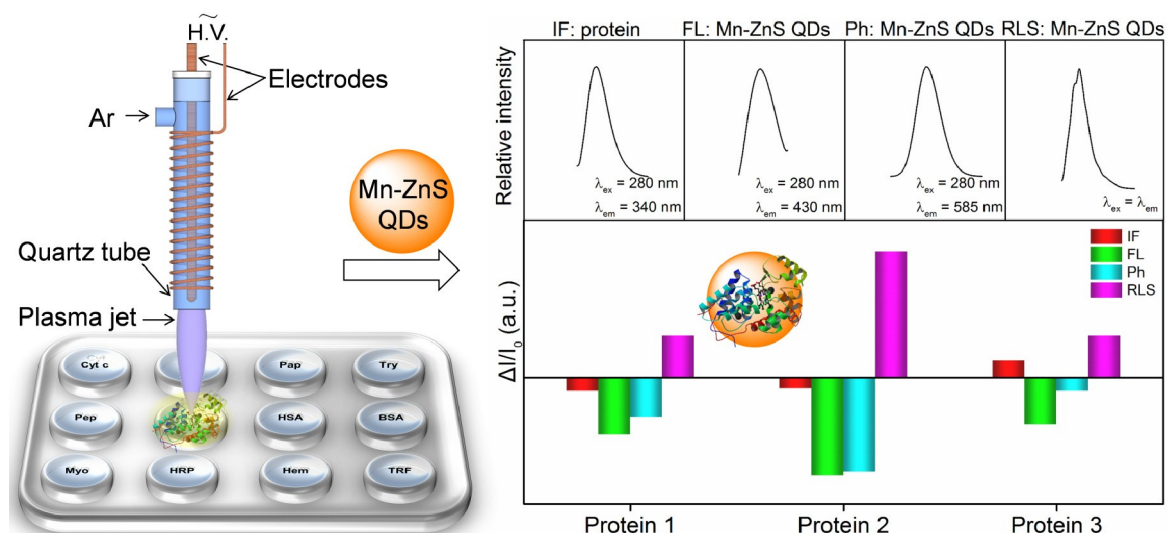
Extraction of multidimensional/multimodal information from a given analytical system provides a robust approach for rapid, sensitive and high-throughput detection.<sup>1-6</sup> By definition, single modal analytical devices are only able to capture information about a single domain, which is often suffered by noisy sensor data, non-universality and/or lack of distinctiveness of the sensor moiety, and even spoof attacks. In contrast, ideally orthogonal or independent signal (especially originated from different physical properties) can be extracted from a multidimensional/multimodal sensing device,<sup>7</sup> thus enriching the information and strengthening the analytical capacity by increasing the measurement or feature space dimensionality. The enriched information is expected to be helpful to large-scale proteomics.

Multidimensional/multimodal sensors have attracted great attention because they are able to provide multidimensional information from an individual sensor element,<sup>8</sup> which are known as “lab-on-a-molecule” or “lab-on-a-nanoparticle”.<sup>9</sup> Compared with single-mode analytical devices, multidimensional sensor devices can largely alleviate the trade-off between molecular sensitivity and dynamic range, since different sensor elements target different analyte concentration regime.<sup>10, 11</sup> Considering that the modern bio-nano-interaction is a multiphysics process, nanocrystal-based biosensors can thus simultaneously generate absorption, fluorescence, mass, and electric perturbations, to name just a few commonly measured signals. In this respect, a series of nanocrystals, such as quantum dots (QDs),<sup>12-15</sup> graphene,<sup>4, 16</sup> Eu-doped TiO<sub>2</sub> nanoparticles,<sup>17-19</sup> have been used

for signaling. Among all of them, optical readout possesses the advantages of easy information collection and simple sensing device fabrication. In this regard, absorption, fluorescence, phosphorescence, polarization, and Rayleigh light scattering, are all potential signal transduction modes for constructing of multimodal sensing devices, but to date only bimodal<sup>15, 17, 19</sup> or tri-modal<sup>3, 12-14</sup> optical information has been utilized in reported biosensors. It is still a challenge to extract more dimensional optical information from a single system for high-order sensing.

The intrinsic fluorescence (IF) of proteins has long been considered as an effective tool for studying protein structure and dynamics,<sup>20</sup> but seldom for protein recognition analysis, probably because the IF is majorly originated from the tryptophan residues, resulting in limited specificity for a given protein. Besides, it also contributes to the fluorescence background in bioanalysis. Since the fluorescence from the tryptophan residues is their location microenvironment-dependent, the IF can be explored as a signal input for multidimensional protein optosensing device to rich the extracted information and increase the discrimination capability. For differential sensing, increasing the cross-reactivity of individual sensor element is an effective tool for boosting the discrimination capacity.<sup>21-23</sup> The interactions between plasmas and biomolecules have been proposed to modify the structure and change the bioactivities of biomolecules.<sup>24-29</sup> Accordingly, here we proposed the use of dielectric barrier discharge (DBD) plasma for protein modification to amplify the cross-reactivity of the IF in multidimensional optosensing device (Scheme 1) for improved proteins recognition and discrimination.

Therefore, we report a quadruple-channel optosensing device



**Scheme 1.** Schematic illustration of the plasma-assisted quadruple-channel optosensing device based on simultaneous exploration of the IF of proteins and the triple-channel optical properties (FL, Ph and RLS) of Mn-doped ZnS QDs for proteins discrimination. Protein samples were first treated with the low-temperature DBD plasma and then the IF of proteins was obtained. After incubation with proteins, the changes of the triple-channel optical information of Mn-doped ZnS QDs were collected. In this manner, the quadruple-channel optical outputs of the multidimensional optosensing device were integrated to better display the "fingerprints" for proteins, which were then subjected to statistical analysis for protein discrimination and recognition. Protein 1, protein 2 and protein 3 represent three random proteins among the twelve proteins. The low-temperature DBD plasma condition: Ar gas flow rate was 600 mL min<sup>-1</sup>; the input voltage between two electrodes was 150 V; the distance between the end of the quartz tube and the surface of the protein solution was 10 mm; and each protein was exposed to the plasma for 5 min.

for proteins, based on simultaneous extracting the IF of proteins and the triple-channel optical information from Mn-doped ZnS quantum dots (QDs)<sup>12-14</sup> during their interactions (Scheme 1). Upon excitation at 280 nm, proteins fluoresce at 340 nm (channel 1, IF), while Mn-ZnS QDs emit fluorescence at 430 nm (channel 2, the defect-related emission of ZnS) and phosphorescence at 585 nm (channel 3, dopant emission of Mn<sup>2+</sup> due to <sup>4</sup>T<sub>1</sub> → <sup>6</sup>A<sub>1</sub> triplet transition). The fourth channel optical information is obtained from the Rayleigh light scattering of Mn-ZnS QDs, which is strengthened when aggregation of QDs occurs. These four channels of optical signal were integrated for differential sensing of proteins. Compared with using triple-channel optical information from Mn-ZnS QDs only,<sup>12-14</sup> the proposed plasma-assisted quadruple-channel optosensing dramatically improved the discrimination resolution and precision for proteins in biological samples and cell lysates.

## Results and discussion

Twelve common proteins with diverse structural characteristics (Table 1), namely metal/nonmetal-containing proteins, molecular weights (MW) and isoelectric points (pI), were randomly chosen to illustrate our proof of concept. After plasma treatment (see the Supporting Information for details), the IF of the proteins was collected and the proteins were then subjected to interact with Mn-doped ZnS QDs. As shown in Fig. 1a, the presence of the analyte proteins (50 nM) resulted in varied IF, FL, Ph and RLS responses, i.e., the fingerprints of these proteins. By linear discriminant analysis (LDA),<sup>30</sup> these proteins were successfully clustered into twelve groups that correspond to each specific protein (95% confidence ellipses), i.e., 100% accuracy according to the jack-knifed classification matrix - that removes and replaces one case at a time (cross-validation routine) (Table S2-

S5<sup>†</sup>). LDA converts the patterns of the training matrix (4 channels × 12 proteins × 5 replicates) to four canonical scores (96.58%, 3.00%, 0.33%, 0.09%) and the first two most significant discrimination factors were used to generate a 2D canonical score plot (Fig. 1b). The detection and discrimination efficiency were validated through identification of 60 unknown protein samples randomly taken from the training set, with 100% accuracy achieved (Table S6).

**Table 1.** Basic properties of the target proteins.

Protein	Abbreviation	Metal	pI	MW (kDa)
Cytochrome c	Cyt c	Yes	10.7	12.3
Lysozyme	Lys	No	11.0	14.4
Papain	Pap	No	9.6	23
Trypsin	Try	No	10.5	24
Pepsin	Pep	No	1-2.5	35
Egg white albumin	EA	No	4.6	45
Human serum albumin	HSA	No	5.2	69.4
Bovine serum albumin	BSA	No	4.8	66.3
Myoglobin	Myo	Yes	7.2	17
Horseradish peroxidase	HRP	Yes	5.0	40
Hemoglobin	Hem	Yes	6.8	64.5
Transferrin	TRF	Yes	5.6	75

### 50 Evaluation of the contribution of IF to the multidimensional optosensing device

The introduction of IF to the multidimensional optosensing device substantially improved the minimal concentration of proteins that can be discriminated by one-order of magnitude, as compared to that without the introduction of the IF.<sup>12</sup> Experimentally, we observed heavy overlap of proteins at 50 nM in the canonical score plot (either with or without the plasma-treatment), when using the triple-channel sensor (FL, Ph and RLS from Mn-doped ZnS QDs, Fig. S5<sup>†</sup>). It is expected that the

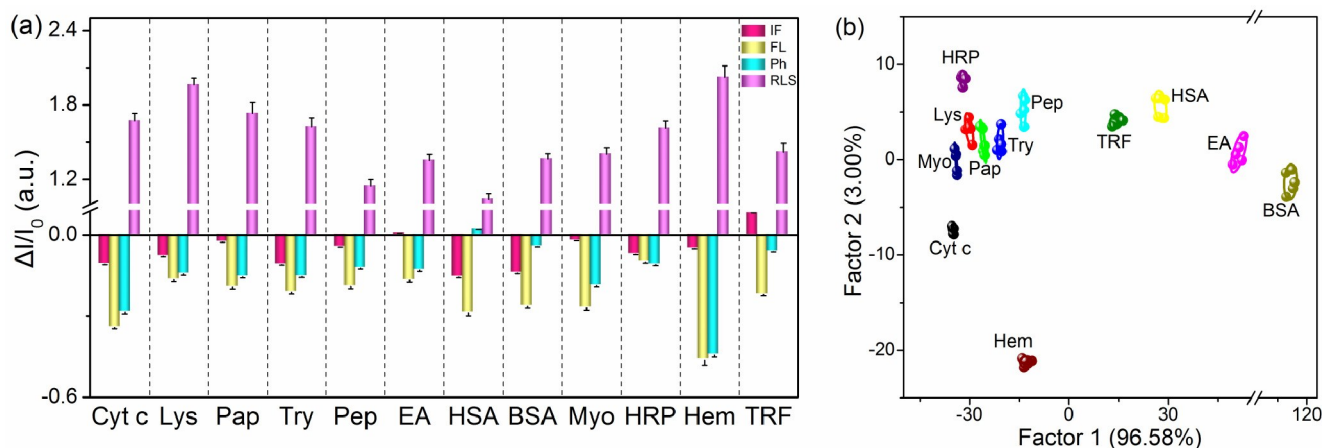


**Fig. 1** Differential sensing of twelve proteins at a concentration of 50 nM. (a) Fingerprints for each protein generated from IF, FL, Ph and RLS response patterns; and (b) canonical score plot (with 95% confidence ellipses) for the IF, FL, Ph and RLS patterns obtained from LDA against twelve proteins with plasma treatment.

5 incorporation of the IF of proteins would increase the measurement or feature space dimensionality of the multidimensional optosensing device, leading to improved orthogonality and thus much better discrimination. Even when the protein concentrations were 25 nM, the majority of the  
 10 proteins could still be successfully discriminated with the proposed quadruple-channel optosensing device, except for HRP and Myo, EA and HSA slightly overlapped in the canonical score plot (Fig. S6<sup>†</sup>).

To identify the exact contribution of IF in discrimination of  
 15 proteins, the protocol developed by Anzenbacher et al.<sup>31</sup> based on principal component analysis (PCA) was employed here and the results were given in Fig. 2. The PCA score plots presented here utilized the first three principal components (PCs) that represented at least 95% of variance. It is evident that each of the  
 20 quadruple-channel optical input all contribute significantly to the discrimination, as evidenced from their contributions to each individual PC. To guarantee sufficient discrimination resolution, none of them can be simply discarded. As expected, the IF was identified as one of the most important contributors. For example,  
 25 at protein concentration of 50 nM, the contribution ratios of IF to PC1, PC2 and PC3 were 16.94%, 38.11% and 39.58%, respectively. None of these ratios represented the lowest contributions to each individual PC. For other protein concentrations, the contribution of IF even is the highest among  
 30 one of PCs. Therefore, these data clearly demonstrate the significance of the IF in the proposed multidimensional optosensing device for protein sensing. However, it is evident that LDA gave better discrimination resolution than PCA, and we thus took LDA throughout this work.

### 35 Confirmation of the plasma modification to proteins.

Introduction of the DBD plasma for protein sample treatment increased the differences among proteins before interaction with Mn-ZnS QDs. A low-temperature DBD plasma jet with Ar as the discharge gas<sup>32, 33</sup> was utilized for protein treatment. Compared to  
 40 the plasma treated case (Fig. 1b), the discrimination resolution of the quadruple-channel optosensing device without plasma treatment was not satisfied since the overlap between HRP and Myo (also Pep and Try) existed (Fig. S7<sup>†</sup>, marked in the gray

square). The discharge conditions were investigated by detecting  
 45 IF, FL, Ph and RLS intensity for best discrimination (Fig. S4<sup>†</sup>).

The structural changes of proteins induced by the plasma jet were studied with circular dichroism (CD), UV-vis absorption, intrinsic fluorescence, time-resolved fluorescence decay, and polyacrylamide gel electrophoresis (PAGE). These spectra of Cyt c before and after plasma treatment were given in Fig. 3 and the rest were given in Fig. S8-S11<sup>†</sup> in the Supporting Information. The far-UV CD spectra of Cyt c revealed clear change of the secondary structure after the treatment (Fig. 3a). Further analysis of the CD spectra with the “Dicroprot” software indicated the  $\alpha$ -  
 55 helix,  $\beta$ -sheet,  $\beta$ -turn and random coil of these proteins changed considerably (Table S8<sup>†</sup>). However, there were still CD signals of secondary structure after plasma treatment, indicating that the relatively mild plasma conditions did not induce complete loss of the secondary structures of proteins. Similar to the CD spectra,  
 60 appreciable change in the UV-vis absorption spectra was observed and the characteristic  $\gamma$ -band absorption of Cyt c was lost greatly (Fig. 3b), probably due to breakage of the Fe-porphyrin structure but no significant molecular weight change (Fig. S12<sup>†</sup>). Meanwhile, the IF of Cyt c was quenched somewhat  
 65 (Fig. 3c), accompanied by shortened fluorescence decay (Fig. 3d), which implied changes of microenvironment of tryptophan residues in Cyt c. It has been reported that plasma could cause denaturation of proteins due to the break of aromatic amino acids or disulfide groups in the protein structure.<sup>34</sup> Therefore, the  
 70 observed spectra change here should be also ascribed to plasma treatment. For other proteins, changes of CD, UV-vis, IF, and fluorescent decay were similar for proteins possessing similar structures (for example, Cyt c, Myo, HRP and Hem all have metal-containing porphyrin units; HSA and BSA are both  
 75 albumins). Consequently, it could be concluded that the optical signal change of the protein-Mn-ZnS system results from the subtle nuance of proteins upon the plasma treatment (Fig. S13-S17<sup>†</sup>).

Protein denaturing can be induced with a variety of approaches,  
 80 such as UV irradiation and heating. We thus compared the effects of these protein modification schemes with this plasma treatment. As shown in Fig. S18<sup>†</sup>, neither UV irradiation nor heating could effectively aid the discrimination of proteins as that of the plasma

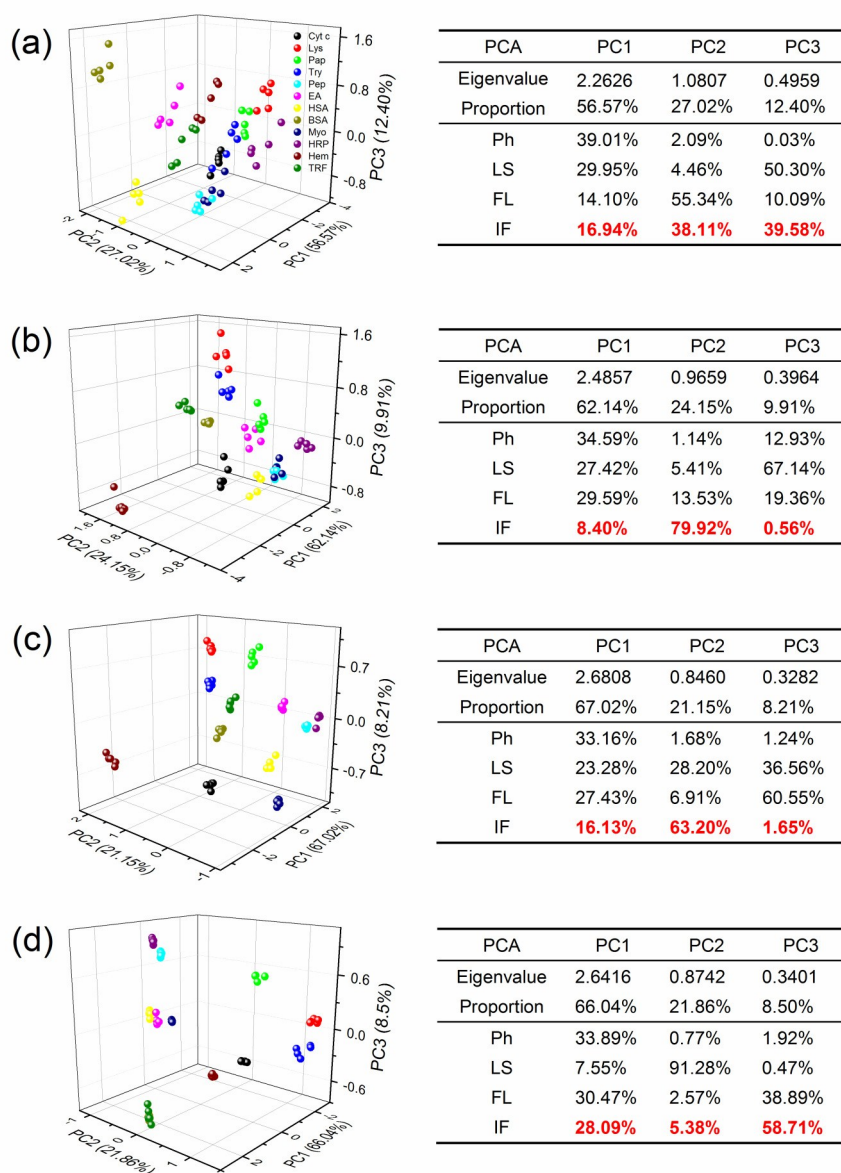


**Fig. 2** Evaluation of the contributions of the quadruple-channel optical inputs in the multidimensional optosensing device for protein discrimination at various concentrations (a: 50 nM; b: 100 nM; c: 250 nM; and d: 500 nM) through the protocol developed by Anzenbacher et al.<sup>13</sup> The left panel shows the PCA score plots for clustering of the 12 proteins and the right panel summarizes the statistical contributions of each optical input. The eigenvalue is a number that tells how much variance in the data in that direction, while the proportion indicates the contribution of each PC to the overall discrimination. Both the eigenvalue and the proportion of each PC were evaluated via eigenanalysis. The sum of the contributions of Ph, LS, FL and IF to each PC is 100%.

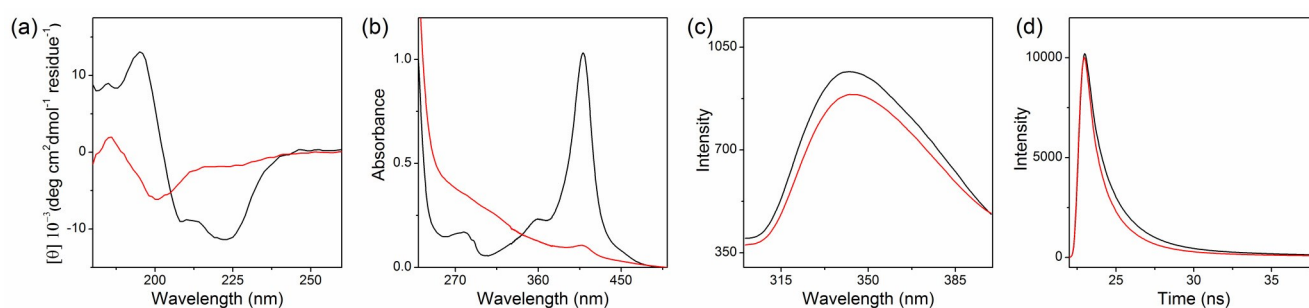


**Fig. 3** Confirmation of the plasma-induced protein structure change of Cyt c: (a) CD; (b) UV-vis; (c) IF; and (d) fluorescence decay. The black and red lines show the corresponding spectra of Cyt c before and after the plasma treatment.

treatment, confirming the unique role of the plasma treatment in the proposed multidimensional optosensing device for proteins. It is well-known that the electrons (typically  $1-10^{10}$  eV) in a DBD plasma can excite the surrounding gas to generate energetic radicals. A variety of reactive radicals were thus identified from the emission spectrum of the Ar plasma jet (Fig. 4), such as  $\cdot\text{OH}$  (283 and 309 nm,  $\text{A}^2\Sigma^+ \rightarrow \text{X}^2\Pi^+$ ),  $\cdot\text{N}_2$  (316, 358 and 380 nm,  $\text{C}^3\Pi_u \rightarrow \text{B}^3\Pi_g$ ) and  $\cdot\text{NH}$  (336.0 nm,  $\text{A}^3\Pi \rightarrow \text{X}^3\Sigma$ ).<sup>35</sup> It is expected that these radicals together with electrons in the DBD plasma caused inactivation and/or re-arrangement of the amino acid residues in the proteins, thus amplifying the difference among the proteins and better discrimination resolution.

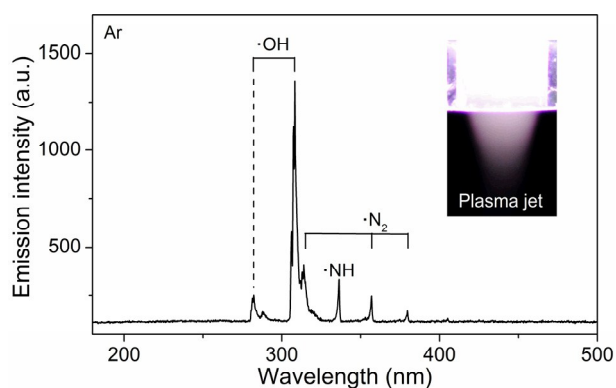


**Fig. 4** Optical emission spectrum of the Ar DBD plasma jet. The inset shows the photograph of the plasma.

#### Application of the multidimensional optosensing device for detection of a given protein at varied concentrations.

After successful discrimination of the target proteins, the next challenge was to detect a protein at various concentration levels. Taking BSA as a model, we demonstrated that the proposed quadruple-channel optosensing device was able to identify BSA of different concentrations. The LDA plots for various concentrations of BSA were not random, but rather followed certain patterns and so can be differentiated from each other in the concentration range of 10-500 nM (Fig. 5a). Notably, the first canonical score was higher than 99%, and it was thus possible to simply use Factor 1 for protein identification and quantification. The linear responses of the canonical score *versus* the concentration (Fig. 5b) allowed simultaneously qualitative and quantitative analysis of proteins.

#### Application of the multidimensional optosensing device for detection of mixtures of proteins.

Next, we investigated the detection of mixed serum proteins with the proposed 50/50/0, 50/0/50, 0/50/50, and 33/33/33 with 100 nM of total proteins) and were tested against the optosensing device. When subjected to the LDA analysis, the canonical score plots resolved these mixtures clearly (Fig. 6). Although no clear evidence to draw the correlation between the plots, such investigation still indicated that the profiles of protein mixtures can be generated, and this would be potentially useful for detection of some disease states that feature altered levels of proteins.

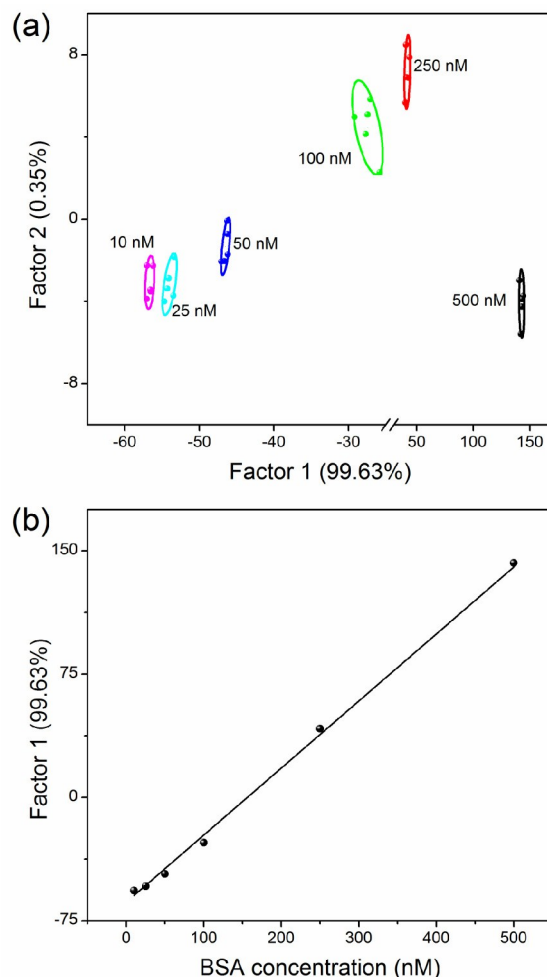


**Fig. 5** (a) Canonical score plot for the quadruple-channel patterns obtained from the LDA against different concentrations of BSA (10 nM, 25 nM, 50 nM, 100 nM, 250 nM and 500 nM, with 95% confidence ellipses); and (b) linear plot of the first discriminant factor vs. the BSA concentrations.

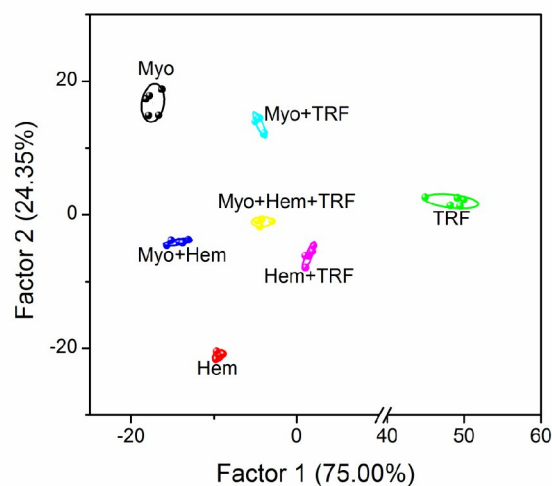


**Fig. 6** Canonical score plot for the quadruple-channel patterns obtained from the LDA against protein mixtures, with 95% confidence ellipses.

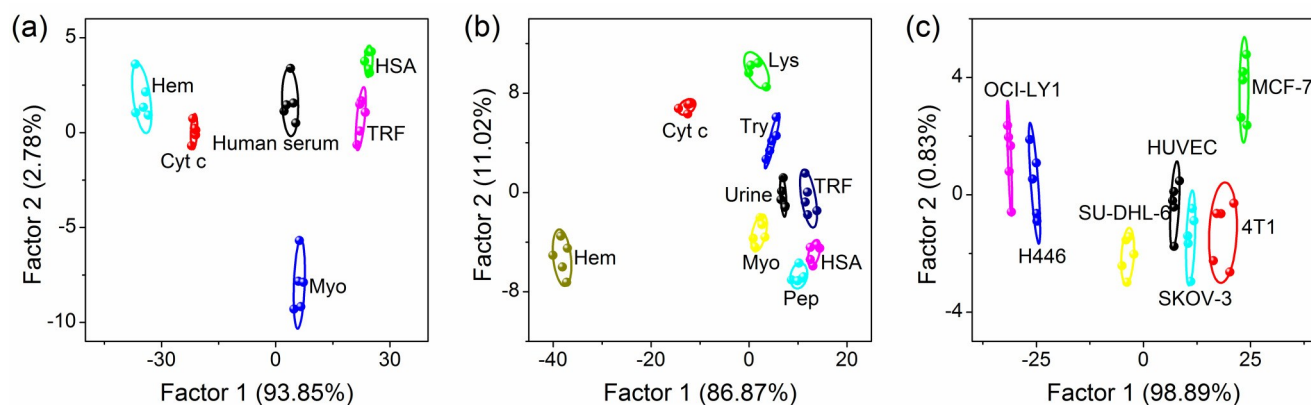


**Fig. 7** Investigation of the performance of the proposed quadruple-channel optosensing device for proteins identification in human serum and human urine and sensing of cells: (a) canonical score plot for the quadruple-channel patterns as obtained from the LDA against human serum; (b) canonical score plot for the quadruple-channel patterns as obtained from the LDA against human urine; and (c) canonical score plot for the quadruple-channel patterns as obtained from the LDA against seven cell lines. The density of each cell suspension is set at 50 000 cells/mL.

### Application of the multidimensional optosensing device for detection of proteins in human serum, urine and cell lysates.

The performance of the quadruple-channel optosensing device was further investigated for detection of proteins in human serum and urine. Both serum and urine are characterized as a complex matrix with high overall protein and electrolyte contents, thus rather challenging for the identification of proteins. We spiked physiologically relevant proteins (50 nM) in human serum and human urine, and analyzed with the quadruple-channel sensing device. As shown in Fig. 7a and 7b, five proteins in human serum and eight proteins in human urine were both completely distinguished with 100% accuracy. These results indicated that this optosensing device held great promise for the discrimination of proteins in a biological matrix.

Lastly, we studied whether such quadruple-channel optosensing device could be used for discrimination of different types of cell lines, including normal, cancerous, and metastatic ones, since cell detection is important for diagnosis of cancers.<sup>36, 37</sup> Three different types of cell lines including human normal cell (HUVEC), human cancerous cell (MCF-7, H446, SKOV-3, OCI-LY1, SU-DHL-6), and mouse metastatic cell (4T1) were randomly selected as the targets. After lysis, proteins inside the cells were extracted and used for discrimination. As shown in Fig. 7c, after the LDA, the different cell types are clustered into seven well resolved groups (95% confidence level ellipses), demonstrating the analytical potential of the quadruple-channel optosensing device for differentiation between normal, cancerous, and metastatic cells as well as different cancer cell types.

### Conclusions

In summary, we have developed a quadruple-channel optosensing device for protein analysis, based on simultaneous exploration of the triple-channel optical properties of Mn-ZnS QDs (FL, Ph, RLS) and the IF of proteins as the fourth channel. The introduction of IF to the multidimensional optosensing device dramatically improved the minimal concentration of proteins that can be discriminated by one-order of magnitude, as compared to that without the IF channel.<sup>12</sup> Notably, introduction of low-temperature atmospheric DBD plasma for protein

treatment substantially increased the cross-reactivity of the quadruple-channel optosensing device and thus discrimination capacity. The throughput of the plasma treatment could be further improved via the use of array plasmas (Fig. S20†). Applications of the quadruple-channel optosensing device were demonstrated for discrimination of proteins in human urine and serum samples, and also proteins of different concentration levels and mixtures. Furthermore, the utilization of such optosensing device for discrimination of different types of cell lines was successful. Future application of this multidimensional optosensing device can be expected for discriminating the progression of different cancer states in a specific cell line and even different cancerous tissues.<sup>37, 38</sup>

### Acknowledgement

The authors gratefully acknowledge the financial support from the National Natural Science Foundation of China (Grants 20835003, 21205084, and 21522505) and the National High Technology Research and Development Program of China (No. 2013AA031901).

### Notes and references

Key Lab of Green Chemistry and Technology of Ministry of Education, College of Chemistry, and Analytical & Testing Center, Sichuan University, Chengdu 610064, China. E-mails: houxd@scu.edu; wupeng@scu.edu.cn; Tel: +86-(28)-8541 0518; +86-(28)-8547 0818  
† Electronic Supplementary Information (ESI) available: Fig. S1-S20; Tables S1-S12, and full experimental details and procedures. See DOI: 10.1039/b000000x/

- 1 P. M. Kosaka, PiniV, J. J. Ruz, R. A. da Silva, M. U. González, D. Ramos, M. Calleja and J. Tamayo, *Nat. Nanotechnol.*, 2014, **9**, 1047-1053.
- 2 J. Park, D. Bang, K. Jang, E. Kim, S. Haam and S. Na, *Nat. Commun.*, 2014, **5**, 3456.
- 3 Y. Y. Lin, R. Chapman and M. M. Stevens, *Anal. Chem.*, 2014, **86**, 6410-6417.
- 4 A. Y. Zhu, F. Yi, J. C. Reed, H. Zhu and E. Cubukcu, *Nano Lett.*, 2014, **14**, 5641-5649.
- 5 S. J. Xie, Y. X. Lu, S. C. Zhang, L. D. Wang and X. R. Zhang, *Small*, 2010, **6**, 1897-1899.

- 6 S. Sax, E. Fisslthaler, S. Kappaun, C. Konrad, K. Waich, T. Mayr, C. Slugovc, I. Klimant and E. J. W. List, *Adv. Mater.*, 2009, **21**, 3483-3487.
- 7 K. Galkowski and N. P. Karampetakis, *Multidimens. Syst. Sign. Process.*, 2012, **23**, 1-3.
- 8 A. Hierlemann and R. Gutierrez-Osuna, *Chem. Rev.*, 2008, **108**, 563-613.
- 9 K. Chen, Q. Shu and M. Schmittel, *Chem. Soc. Rev.*, 2014, **44**, 136-160.
- 10 M. Schmittel and H. W. Lin, *Angew. Chem. Int. Ed.*, 2007, **46**, 893-896.
- 11 Q. J. Zhang, Z. C. Zhu, Y. L. Zheng, J. G. Cheng, N. Zhang, Y. T. Long, J. Zheng, X. H. Qian and Y. J. Yang, *J. Am. Chem. Soc.*, 2012, **134**, 18479-18482.
- 12 P. Wu, L.-N. Miao, H.-F. Wang, X.-G. Shao and X.-P. Yan, *Angew. Chem. Int. Ed.*, 2011, **50**, 8118-8121.
- 13 L.-J. Sang and H.-F. Wang, *Anal. Chem.*, 2014, **86**, 5706-5712.
- 14 L.-J. Sang, Y.-Y. Wu and H.-F. Wang, *ChemPlusChem*, 2013, **78**, 423-429.
- 15 P. Wu, T. Zhao, Y. F. Tian, L. Wu and X. D. Hou, *Chem. Eur. J.*, 2013, **19**, 7473-7479.
- 16 Y. X. Lu, H. Kong, F. Wen, S. C. Zhang and X. R. Zhang, *Chem. Commun.*, 2013, **49**, 81-83.
- 17 J. Hu, X. M. Jiang, L. Wu, K. L. Xu, X. D. Hou and Y. Lv, *Anal. Chem.*, 2011, **83**, 6552-6558.
- 18 W. Y. Xie, W. T. Huang, J. R. Zhang, H. Q. Luo and N. B. Li, *J. Mater. Chem.*, 2012, **22**, 11479-11482.
- 19 D. Liu, M. Y. Liu, G. H. Liu, S. C. Zhang, Y. Y. Wu and X. R. Zhang, *Anal. Chem.*, 2010, **82**, 66-68.
- 20 M. L. Saviotti and W. C. Galley, *Proc. Nat. Acad. Sci. USA*, 1974, **71**, 4154-4158.
- 21 J. P. Anzenbacher, P. Lubal, P. Bucek, M. A. Palacios and M. E. Kozelkova, *Chem. Soc. Rev.*, 2010, **39**, 3954-3979.
- 22 E. V. Anslyn and V. M. Rotello, *Curr. Opin. Chem. Biol.*, 2010, **14**, 683-684.
- 23 K. J. Albert, N. S. Lewis, C. L. Schauer, G. A. Sotzing, S. E. Stitzel, T. P. Vaid and D. R. Walt, *Chem. Rev.*, 2000, **100**, 2595-2626.
- 24 M. Laroussi, *IEEE Trans. Plasma Sci.*, 2002, **30**, 1409-1415.
- 25 M. Laroussi, *Plasma Process. Polym.*, 2005, **2**, 391-400.
- 26 O. Volotskova, T. S. Hawley, M. A. Stepp and M. Keidar, *Sci. Rep.*, 2012, **2**, 636.
- 27 H. M. Joh, J. Y. Choi, S. J. Kim, T. H. Chung and T.-H. Kang, *Sci. Rep.*, 2014, **4**, 6638.
- 28 H. Yasuda, M. Hashimoto, M. M. Rahman, K. Takashima and A. Mizuno, *Plasma Process. Polym.*, 2008, **5**, 615-621.
- 29 E. Takai, K. Kitano, J. Kuwabara and K. Shiraki, *Plasma Process. Polym.*, 2012, **9**, 77-82.
- 30 P. C. Jurs, G. A. Bakken and H. E. McClelland, *Chem. Rev.*, 2000, **100**, 2649-2678.
- 31 M. A. Palacios, Z. Wang, V. A. Montes, G. V. Zyryanov and P. Anzenbacher, *J. Am. Chem. Soc.*, 2008, **130**, 10307-10314.
- 32 X. M. Jiang, Y. Chen, C. B. Zheng and X. D. Hou, *Anal. Chem.*, 2014, **86**, 5220-5224.
- 33 W. Li, C. B. Zheng, G. Y. Fan, L. Tang, K. L. Xu, Y. Lv and X. D. Hou, *Anal. Chem.*, 2011, **83**, 5050-5055.
- 34 B. Surowsky, A. Fischer, O. Schlueter and D. Knorr, *Innov. Food Sci. Emerg.*, 2013, **19**, 146-152.
- 35 G. Herzberg, *The spectra and structures of simple free radicals: an introduction to molecular spectroscopy*, Dover Publications, Mineola, N.Y., 2003.
- 36 A. Bajaj, O. R. Miranda, I. B. Kim, R. L. Phillips, D. J. Jerry, U. H. F. Bunz and V. M. Rotello, *Proc. Natl. Acad. Sci. U. S. A.*, 2009, **106**, 10912-10916.
- 37 A. Bajaj, O. R. Miranda, R. Phillips, I. B. Kim, D. J. Jerry, U. H. F. Bunz and V. M. Rotello, *J. Am. Chem. Soc.*, 2010, **132**, 1018-1022.
- 38 S. Rana, A. K. Singla, A. Bajaj, S. G. Elci, O. R. Miranda, R. Mout, B. Yan, F. R. Jirik and V. M. Rotello, *ACS Nano*, 2012, **6**, 8233-8240.